

X-ray photoelectron spectroscopy analysis of ion-beam-induced oxidation of GaAs and AlGaAs

J. L. Alay

Interuniversitair Micro-Elektronica Centrum vzw (IMEC), Kapeldreef 75, B-3001 Leuven, Belgium, and Laboratori de Caracterització de Materials per la Microelectrònica, Universitat de Barcelona, Avda. Diagonal 645, 08028 Barcelona, Spain

W. Vandervorst

Interuniversitair Micro-Elektronica Centrum vzw (IMEC), Kapeldreef 75, B-3001 Leuven, Belgium

(Received 12 December 1991; accepted 6 April 1992)

The oxidation of GaAs and AlGaAs targets subjected to O_2^+ bombardment has been analyzed, using *in situ* x-ray photoelectron spectroscopy, as a function of time until steady state is reached. The oxides formed by the O_2^+ bombardment have been characterized in terms of composition and binding energy. A strong energy and angular dependence for the oxidation of As relative to Ga is found. Low energies as well as near normal angles of incidence favor the oxidation of As. The difference between Ga and As can be explained in terms of the formation enthalpy for the oxide and the excess supply of oxygen. In an AlGaAs target the Al is very quickly completely oxidized irrespective of the experimental conditions. The steady state composition of the altered layers show in all cases a preferential removal of As.

I. INTRODUCTION

In order to achieve very high sensitivities, it is common practice in secondary-ion mass spectroscopy (SIMS) analysis to use oxygen as the primary ion. The incorporation of the oxygen ions in the target leads to a strong oxidation and induces drastic enhancements of the secondary-ion yields of the sputtered species.¹ In addition, the resulting compound formation can lead to serious redistribution phenomena such as impurity segregation. Therefore, a detailed evaluation of the interaction between the target and the bombarding species is required in order to understand and model the basics of SIMS analysis.

It should be noted, however, that, although the ion-beam-induced oxidation is discussed here from the SIMS perspective, the results on the oxide growth and dynamics have a wider applicability and are also of use in the more general case of insulator growth by ion beams. A study on ion beam oxidation of Si (Ref. 2) has indeed shown the applicability of the simple ion retention model during sputtering but also emphasized the importance of compound formation.³ The objective of this investigation was to extend this work to III-V materials and analyze the ion-beam-induced oxidation of GaAs and $Al_{0.8}Ga_{0.2}As$ targets under O_2^+ bombardment, as occurring during SIMS analysis. In this respect we have determined the surface stoichiometry of the built-up oxides, the dynamics of the oxide growth, and the stoichiometry of the underlying layers.

Compared to the ion-beam oxidation of Si, the situation of III-V materials is much more complex since one has now not only to consider the degree of oxidation but also eventual preferential removal or oxidation of one of the constituents of these targets. For instance, it is widely known that the Al of AlGaAs shows a very strong oxidation after exposure to atmosphere, an effect which could be persistent during ion-beam oxidation. No previous results on the ion-beam oxidation of AlGaAs have been reported.

Previous work on ion-beam oxidation of GaAs has indicated that Ga is preferentially oxidized with respect to As and that the degree of preferential oxidation is strongly energy dependent.^{4,5} Whereas in the previous work the final state was considered for normal incidence only, in this paper we explore the complete dynamics of this oxide growth for different energies and angles of incidence. Attention is also paid to a quantitative investigation of the in-depth distribution of the different elements and their chemical bonding using *in situ* (angular resolved) x-ray photoelectron spectroscopy (XPS).

II. EXPERIMENTAL

The molecular-beam epitaxy (MBE) grown GaAs (100) and $Al_{0.8}Ga_{0.2}As$ samples were bombarded with an O_2^+ ion beam with energies ranging from 0.5 to 5 keV at normal incidence, while rastering over $4 \times 4 \text{ mm}^2$. Due to its special interest, the 1 keV bombardment was carried out at angles of incidence between 0° and 55° , referred to as the target normal. None of the samples was chemically treated prior to the ion-beam bombardments. The Al concentration in the AlGaAs sample has been determined by wavelength dispersive spectroscopy (WDS) with a value of 88%.

In situ XPS data were taken from the center of the rastered area ($4 \times 4 \text{ mm}^2$) with a Surface Science Instrument (SSX-100). This instrument uses monochromatic $AlK\alpha$ radiation ($h\nu = 1486.6 \text{ eV}$) and is equipped with a concentric hemispherical analyzer (CHA) with an acceptance angle of 35° . The base pressure of the analysis chamber is in the 10^{-10} Torr range and rises to 10^{-8} Torr during oxygen bombardment.

Surface chemical composition is based on the Ga 3d, As 3d (fitted for the GaAs peak as a $3d_{3/2}$ and $3d_{5/2}$ doublet), Al 2p, O 1s, and C 1s photoelectron peaks. A good separation between the various chemical states for each

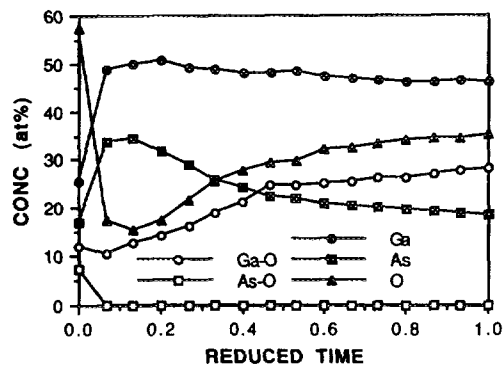


FIG. 1. XPS profile data during O_2^+ bombardment of GaAs (5 keV and normal incidence) as a function of reduced time (described in text) shows gradual Ga oxidation and preferential sputtering of As. Solid symbols refer to the total amount of Ga, As, and O (i.e., oxidized plus metallic peaks), and open symbols to the oxidized fraction only.

element has been established,⁶⁻⁸ so that peak areas can be readily used to determine the fraction of a chemical state in the total photoelectron peak (rel%), within the sampling volume. The concentration profiles are reproduced as a function of the reduced time (rt), which is the ratio between the time of bombardment and the time necessary to reach the steady state. Due to the wide range of photoelectron binding energies [Al 2p (72.65 eV), Ga 3d (18.50 eV), As 3d (40.70 eV), and O 1s (531.50 eV)] being studied in this paper, the corresponding attenuation lengths do not have the same value (33 Å for O 1s and 45 Å for Ga 3d).^{9,10} For this reason the modified Scofield sensitivity factors have been used in order to account for the different sampling depths of the elements. The modified Scofield sensitivity factor for atomic level n [$S_{SF}(n)$] was obtained by multiplying the photoionization Scofield cross sections [$\sigma_{SF}(n)$] by the ratio of escape depths (λ) of the element and C. Assuming an energy dependence¹¹ of the following form, $\lambda \sim kE_K(n)^{0.7}$, this leads to

$$S_{SF}(n) = \sigma_{SF}(n) [E_K(n)/E_K(C\ 1s)]^{0.7}.$$

It should be noted that the latter correction has been derived for profiles with uniform concentrations. For nonuniform structures, deviations might still occur, but these are considered to be too small to be a considerable influence.

III. RESULTS

A. GaAs target

In the case of 5 keV and the normal incidence O_2^+ bombardment, the evolution for the Ga, As, and O species has been studied until the steady state is reached (time of bombardment in which the atomic concentration for all the present species has become constant) (Fig. 1). Before the bombardment starts, the target has a native gallium-arsenic oxide on the surface. Based on the photoelectron binding energy and the total O, Ga, and As concentrations, they can be identified as Ga_2O_3 (46 rel%), As_2O_3 (19 rel%)– As_2O_5 (24 rel%).

After steady state is reached, a thin gallium oxide (61 rel%) is formed with a ratio O/Ga of 1.2 instead of 1.5, which would be required for a stoichiometric gallium oxide (Ga_2O_3). Arsenic oxide is not observed during the whole process except in the native oxide. The binding energy separation between the peak corresponding to the oxide and to the GaAs in the Ga 3d photoelectron region is 1.4 eV for the native oxide, but after bombardment this difference is reduced to 0.9 eV, confirming that the built-up gallium oxide is not perfectly stoichiometric (O/Ga is 1.2 instead of 1.5).

During the bombardment the As as well as the Ga photoelectron peak still show some GaAs components. A quantitative analysis of these components shows a Ga(-As)/As(-Ga) ratio of 1.07 ± 0.1 , in good agreement with a 1:1 GaAs compound. During the incorporation of the oxygen (and the concurrent sputtering of GaAs), the As is gradually being replaced by the oxygen, whereas the Ga concentration remains virtually unchanged. Since no As oxide is detected, all the retained oxygen is bonded to Ga forming the substoichiometric oxide. The total As concentration has now dropped to a value of 18 at. %, much lower than the total Ga concentration (46 at. %). The variations of the total concentrations (oxidized + metallic compounds) as well as the oxidized fractions are summarized in Fig. 1. As compared to the case of Si, there is no sequential replacement of suboxides, but apparently the Ga_2O_3 is formed directly.

Consistent with earlier work,^{4,5} bombardments performed at 2.5, 1.0, and 0.5 keV at normal incidence show an increase in the oxidation of gallium, and the partial formation of arsenic oxide (As_2O_3) for the lower energies (0.5 and 1 keV). The 1 keV bombardment has been studied at different angles of incidence of the ion beam, from normal incidence (0°) to glancing angles (55°) [Fig. 2(a)]. The As oxidation shows a strong dependence with the angle of incidence. At normal or 15° angle of incidence a maximum oxidation level (As_2O_3) is achieved (74 ± 3 rel%), while at 55° the oxidation is practically absent (4.0 rel%). A transition region has been observed at angles ranging from 25° to 35° (65 rel% and 29 rel%). At angles of incidence lower than 25° the As oxide is formed by As_2O_5 and As_2O_3 , with As_2O_3 always being the dominant one, whereas above 25° only As_2O_3 can be found. Ga only shows a weak dependence with the incidence angle, and always has the highest level of oxidation (as much as 81 rel%). Even at 55° , Ga is still predominantly bonded to O (62.5 rel%). The decrease in oxidation ratio of the Ga follows closely the reduced incorporation of oxygen at higher angles [Fig. 2(a)] whereas the As oxidation is decreasing much more strongly. We remark that not only the degree of oxidation is changing but also the total As and Ga concentrations [Fig. 2(b)]. At low angles of incidence the total Ga concentration to total As concentration ratio is 2.6, whereas at 55° it decreases towards 1.8. This decrease is almost solely due to a reduced preferential sputtering of the As at high angles. On the other hand, the ratio Ga(-As)/As(-Ga) corresponding to the GaAs components decreases from 2.1 ± 0.3 for very low angles of inci-

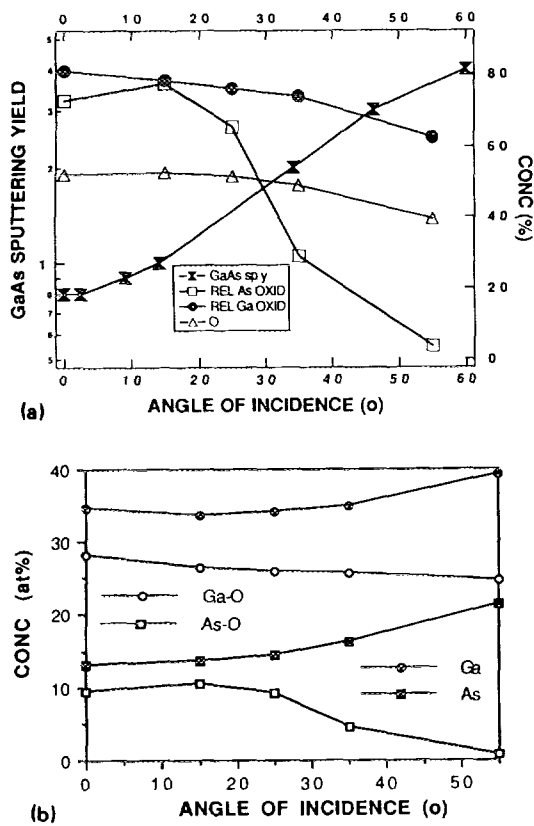


FIG. 2. (a) Relative fraction of oxidation for As and Ga, and total O incorporation in the steady state for 1 keV O₂⁺ bombardment of GaAs target as a function of the angle of incidence. Also shown is the GaAs sputter yield for 10 keV O₂⁺ bombardment. (b) Total amount of As and Ga and total oxidized Ga and As concentrations in the steady state for 1 keV O₂⁺ bombardment on GaAs target as a function of the angle of incidence.

dence to 0.7 ± 0.1 for glancing angles, suggesting that preferential sputtering of As in the sampling depth is very strong at low angles of incidence. Instead of that, at angles near 55°, preferential sputtering is reduced to the near-surface region due to a decrease on the ion penetration depth.

Also shown in Fig. 3(a) is the GaAs-sputter yield (measured for an O₂⁺ ion beam of 10 keV energy^{12,13}) as a function of the angle of incidence. Most experimental data on sputter yields show a similar angular dependence for various energies such that we may assume that the 1 keV data will be quite similar. It is remarkable that the oxygen incorporation hardly shows any correlation with the sputter yield, implying that the incorporation is not dominated by the sputter process (leading to a $1/sy$ dependence for the incorporated ion concentration c_0^3) but probably by some simultaneous interdiffusion. The latter can also be inferred from the fact that despite the low bombardment energy of the oxygen at 1 keV (and hence its low penetration depth) the oxide formed is so thick that virtually no signal from the underlying substrate can be detected.

B. Al_{0.8}Ga_{0.2}As target

A similar study has been performed on an Al_{0.8}Ga_{0.2}As substrate. Figure 3(a) shows the evolution of the total

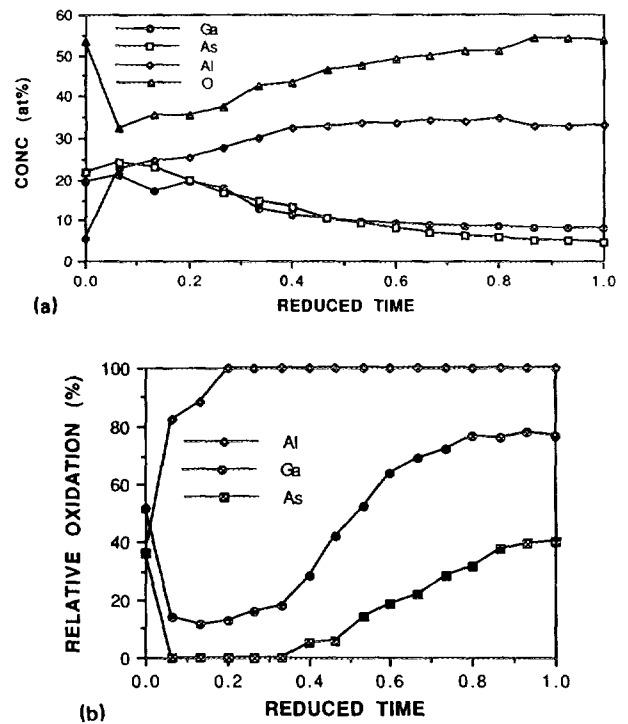
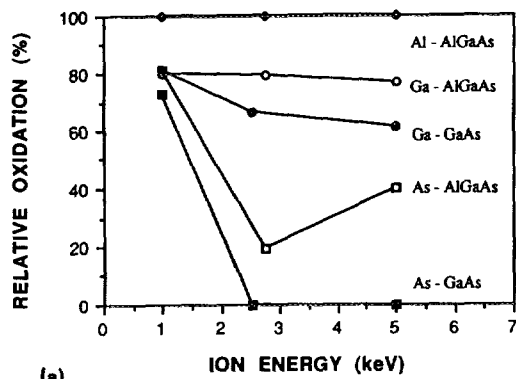


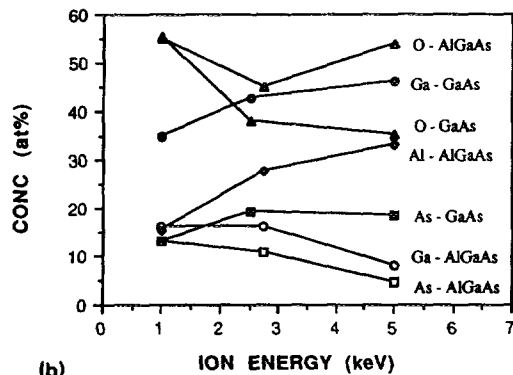
FIG. 3. (a) XPS data profile during O₂⁺ bombardment of AlGaAs (5 keV and normal incidence) as a function of reduced time (described in text) shows preferential sputtering of As relative to Ga and Al. (b) Relative fraction of oxidation for Al, Ga, and As until steady state. (5 keV and normal incidence O₂⁺ bombardment on AlGaAs target.)

different elemental concentrations as well as the incorporated oxygen. The AlGaAs was bombarded with a 5 keV oxygen beam, normally incident. Initially the sample is covered by a native oxide [Al₂O₃ (36 rel%), Ga₂O₃ (52 rel%), As₂O₃ (7 rel%), As₂O₅ (29 rel%)]. The Ga and As oxides are reduced very quickly ($rt = 0.07$) in the first bombardment steps (about 15 rel% for Ga and 0 rel% for As), whereas the Al continuously increases its oxidation level. The Al oxidation is very fast and reaches 100% for $rt = 0.20$, with a ratio O(-Al)/Al(-O) of 1.3 at the end of the bombardment, not far from a ratio of 1.5 corresponding to a stoichiometric Al₂O₃. The binding energy of the oxide peak corresponds to the expected value for Al₂O₃. Only after $rt = 0.20$ can oxidation of Ga and As also be observed. Note also that the total Al content in the surface region keeps increasing from the 5 at. % level for $rt = 0$ up to 33 at. % for $rt = 1$. The very rapid complete oxidation of the Al implies that the incorporated oxygen diffuses rapidly from deeper lying layers (where it was implanted) towards the surface.

For $rt < 0.33$, As remains bonded to Ga and also the oxidation level of Ga stays very low. From $rt > 0.33$, a rapid oxidation takes place for Ga as well as for As. Note that unlike ion-beam oxidation of GaAs, Ga is more oxidized and now As is also oxidized. As forms primarily As₂O₃ and some As₂O₅ in steady state and Ga forms the substoichiometric Ga₂O₃. The substoichiometry again can be inferred from the lower binding energy as compared to Ga₂O₃. The Ga is also more oxidized compared to the GaAs case. The nonoxidized components are no longer



(a)



(b)

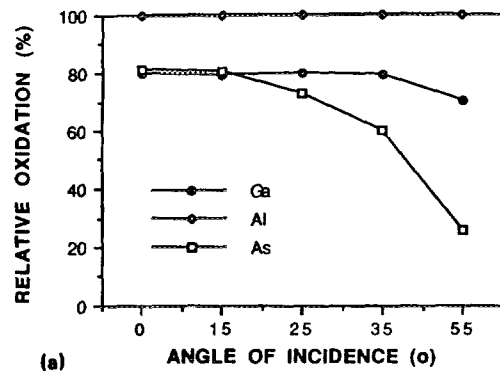
FIG. 4. (a) Relative fraction of oxidation of Al, Ga, and As in GaAs and AlGaAs as a function of the ion energy. (b) Total amount of As, Ga, Al, and O in GaAs and AlGaAs as a function of the ion energy.

stoichiometric GaAs, indicating a preferential sputtering of As. Note also that in the steady state the relative concentrations of Al/Ga/As (7/2/1) are strongly different from the original target composition (4/1/5). In particular, the depletion of As is very pronounced.

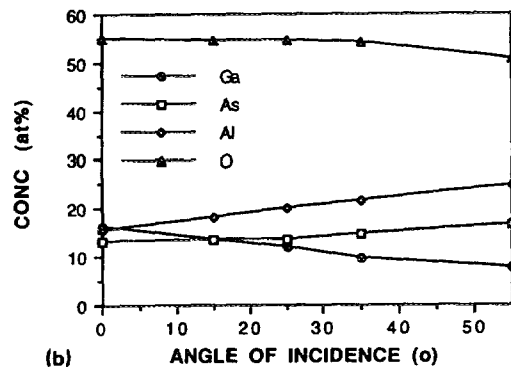
The energy dependence of the oxidation of As and Ga is similar to the results for pure GaAs [Fig. 4(a)]. At low energies a much higher degree of oxidation for the As is observed, rising to an equal level as the Ga for energies around 1 keV. On the other hand, the degree of oxidation of the Ga increases only very slightly at lower energies. The Al is always completely oxidized and shows no energy dependence.

The relative degree of oxidation is not the only parameter changing with energy. The total concentration of Al, As, and Ga in the altered layer is changing as well as the oxygen incorporation [Fig. 4(b)]. Here different trends are found. For GaAs the Ga concentration increases strongly with increasing energy, whereas for AlGaAs a decrease of Ga is found. As also shows a similar behavior. The most dramatic influence is found for the Al, which increases from 15 at. % (for 1 keV) to more than 33 at. % (for 5 keV). Note that in all cases the original stoichiometry of the target is completely lost with a preferential removal of the As in both cases.

Again the angular dependence for a 1 keV bombardment has been studied [Fig. 5(a)]. This is similar to the case of GaAs, where only the relative oxidation degree of As shows a pronounced angular dependence, whereas the



(a)



(b)

FIG. 5. (a) Relative fraction of oxidation of Al, Ga, and As for 1 keV O_2^+ bombardment on AlGaAs target as a function of the angle of incidence in the steady state. (b) Total amount of As, Ga, Al, and O in the steady state for 1 keV O_2^+ bombardment on AlGaAs target as a function of the angle of incidence.

relative oxidation of Ga and Al remains practically unchanged [Fig. 5(a)].

The total concentrations of Al, As, and Ga vary with the angle of incidence [Fig. 5(b)], whereas, in particular, the Al is showing a strong increase for high angles of incidence. Again, it is quite surprising that the amount of oxygen retained is nearly independent of the angle of incidence.

IV. DISCUSSION

The present results indicate that the incorporation of oxygen as a result of ion bombardment of GaAs and AlGaAs targets is not explainable with the simple concept of ion retention during sputtering.³ The latter would imply a steady oxygen concentration inversely proportional with the sputter yield and the formation of very thin oxide layers at low energies. In particular, the angular dependence of the oxygen retention provides evidence for an alternative mechanism since the sputter yield is known to vary quite strongly with the angle and very little variation is found for the oxygen concentration. The thickness of the oxide (about 10 nm) formed at the lowest energies (1 keV) is also much larger than expected based on the projected range of the primary ions (1–2 nm). Both observations indicate that an additional effect is contributing to the oxygen retention. One plausible explanation could be a fast oxygen diffusion beyond the bombarded region, leading to a deeper penetration of the oxygen. Such a (radiation en-

hanced) diffusion could also be the mechanism responsible for the very fast oxidation of the Al in the AlGaAs case. In fact, without such an assumption, not enough oxygen would be available in the near-surface region to explain the observed Al oxidation. An important conclusion, therefore, from the present work is that the simple retention model, although it was found satisfactory for Si,² is not applicable to GaAs and AlGaAs targets.

Other additional differences as compared to Si are of course the effects of preferential sputtering in these multi-element targets. In GaAs as well as AlGaAs we observe a strong preferential sputtering of the As as compared to Ga (and Al). This effect, which appears more pronounced at higher bombardment energies than at low energies, is somewhat reduced at high angles of incidence.

It should also be mentioned that from an (AR) XPS measurement for the 5 keV normal incidence bombardment, one could derive that the Ga and As oxides are distributed uniformly throughout the sampled region, whereas there is a depletion of elemental As towards the surface. The latter is again an indication of the preferential sputtering of As. Another striking feature is the low or retarded oxidation of As as compared to Ga. In GaAs as well as in AlGaAs a strong energy and angular dependence is found in the oxidation degree of the As, whereas the oxidation of Ga seems to be very little influenced. It is clear that a competition between Ga and As for the incorporated oxygen takes place when only a limited supply of oxygen is available. Since the formation enthalpy of the Ga oxide is lower than the one for As oxide,¹⁴ it is expected that Ga will be predominantly oxidized. It is, however, not true that a complete oxidation of Ga is required before As becomes oxidized. In Fig. 6 we show a plot of the relative degree of oxidation of As as a function of the O/(Ga + As) concentration ratio (in the AlGaAs case the O bonded to the Al has been removed before taking the ratio). The data were derived from the angular and the energy dependence, as well as from the variation observed during the buildup of the oxide. From Fig. 6 it is clear that for a given matrix (or Ga/As concentration) the O/(Ga + As) ratio solely determines the relative degree of oxidation of the As. With decreasing the Ga/As ratio the oxidation of As starts at lower O/(Ga + As) ratios, which is understandable since less Ga will be competing for the available oxygen.

V. CONCLUSIONS

The analysis of GaAs and AlGaAs targets during and following oxygen bombardment has shown the preferential oxidation of Ga as compared to As. This effect increases with increasing the bombardment energy and increasing

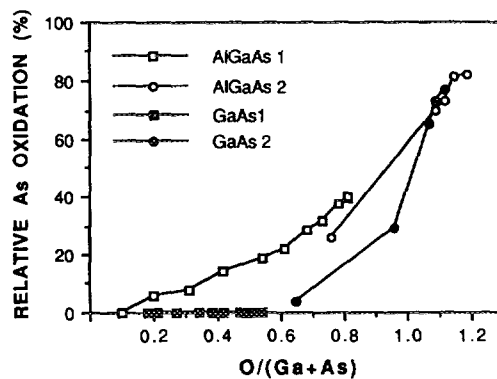


FIG. 6. Relative fraction of oxidation of As for the GaAs and AlGaAs targets as a function of the O/Ga + As ratio, derived from the variation observed during the buildup of the oxide (GaAs 1 and AlGaAs 1) and angular dependence (GaAs 2 and AlGaAs 2).

the angle of incidence. The oxygen concentration measured in the stationary state does not relate to the simple model of ion retention during sputtering but implies a significant indiffusion of the oxygen during irradiation. The latter also leads to a very fast complete oxidation of Al at the initial stages of the bombardment. The difference between As and Ga for oxidation for the different experimental conditions can be qualitatively explained based on the formation enthalpy for the respective oxides and the availability of excess oxygen.

¹F. A. Stevie, P. M. Kahora, D. S. Simons, and P. Chi, *J. Vac. Sci. Technol. A* **6**, 76 (1988).

²J. L. Alay and W. Vandervorst, to be published in 1992 in *Surf. Interface Anal. with ECASIA'91 Conference Proceedings*.

³F. Schultz and K. Wittmaack, *Radiat. Eff.* **29**, 31 (1976).

⁴O. Vancauwenberghe, N. Herbots, H. Mahnoharan, and M. Ahrens, *J. Vac. Sci. Technol. A* **9**, 1035 (1991).

⁵N. Herbots, O. C. Hellman, P. A. Cullen, and O. Vancauwenberghe, in *Deposition and Growth: Limits for Microelectronics*, edited by G. W. by Rubloff, American Vacuum Society Series No. 4, AIP Conf. Proc. 167 (AIP, New York, 1988), p. 259.

⁶G. P. Schwartz, G. J. Gualtieri, G. W. Kammlott, and B. Schwartz, *J. Electrochem. Soc.* **126**, 1737 (1979).

⁷C. D. Wagner, W. M. Riggs, L. E. Davis, J. F. Mulder, and G. E. Muilenberg, *Handbook of X-Ray Photoelectron Spectroscopy* (Perkin-Elmer, Eden Prairie, MN, 1979).

⁸L. A. DeLouise, *J. Appl. Phys.* **70**, 1718 (1991).

⁹S. Tanuma, C. J. Powell, and D. R. Penn, *Surf. Interface Anal.* **17**, 911 (1991).

¹⁰S. Tanuma, C. J. Powell, and D. R. Penn, *Surf. Interface Anal.* **17**, 927 (1991).

¹¹*Practical Surface Analysis by Auger and X-Ray Photoelectron Spectroscopy*, 2nd ed., edited by D. Briggs and M. P. Seah (Wiley, New York, 1990).

¹²K. Wittmaack, *Nucl. Instrum. Methods* **218**, 307 (1983).

¹³K. Wittmaack, *Nucl. Instrum. Methods B* **2**, 674 (1984).

¹⁴Y. Homma and K. Wittmaack, *Appl. Phys. A* **50**, 417 (1990).